

# ON THE PROPERTIES OF THE $^{229}\text{Th}$ ISOTOPE

V. I. Isakov<sup>1</sup>

*Petersburg Nuclear Physics Institute, Gatchina 188300, Russia,*

National Research Centre Kurchatov Institute

## A b s t r a c t

Electromagnetic properties of the deformed neutron-odd nucleus  $^{229}\text{Th}$  are investigated in the framework of the unified model, with primary emphasis upon the properties of the low-lying isomeric state.

On the basis of detailed analysis of  $\gamma$ -transitions in  $^{229}\text{Th}$  attendant  $\alpha$ -decay of  $^{233}\text{U}$ , it was established the existence in the daughter nuclei  $^{229}\text{Th}$  of the low-lying level with the excitation energy of only a few eV. This is the most low-lying state known by now. The next one is the level  $1/2^+$  in  $^{235}\text{U}$ , with the excitation energy equal to 76.5 eV. The latest experimental data [1] point to the value of the excitation energy equal to  $\sim 7.6$  eV. In the paper [2], the authors detected conversion electrons arising from the decay of this level. In this way, they proved that this level really exists, and its energy is above the threshold of ionization of neutral atom of Th, which is equal to  $\sim 6.3$  eV. Together, the half-life of this level equal to  $7(\pm 1)$   $\mu\text{s}$  was measured in [3]. However, the energy of this state is not yet measured in the direct experiment.

Here, we carry out theoretical analysis of the characteristics of  $^{229}\text{Th}$ , and make an attempt to describe decay properties of its low-lying levels, as well as to propose an alternative way for excitation of the above-mentioned state in the reaction of the Coulomb excitation.

In Fig.1 we show experimental scheme of levels and the decay scheme for the low-lying states in  $^{229}\text{Th}$ , that are known by now from the experiment [4, 5]. Here, one can easily observe rotational bands characteristic to the deformed nuclei. Thus, we perform theoretical analysis for this deformed neutron-odd nuclei basing on the ideas of the unified model proposed in the papers [6]– [9].

The wave function of the axially-symmetric odd nuclei in the framework of the unified model reads as

$$\Psi_{MK}^J = \sqrt{\frac{2J+1}{16\pi^2}} \left[ D_{MK}^J(\theta_i) \cdot \chi_K + D_{M-K}^J(\theta_i) \cdot \overline{\chi_K^J} \right]. \quad (1)$$

Second term in (1) provides symmetry of the wave function to reflection relatively the plane orthogonal to the symmetry axis, while

$$\chi_K = \sum_{N\ell\Lambda s} x_K(N\ell\Lambda s) |N\ell\Lambda s\rangle, \quad \overline{\chi_K^J} = \sum_{N\ell\Lambda s} (-1)^{J-\ell-1/2} x_K(N\ell\Lambda s) |N\ell - \Lambda - s\rangle. \quad (2)$$

---

<sup>1</sup>E-mail Visakov@thd.pnpi.spb.ru

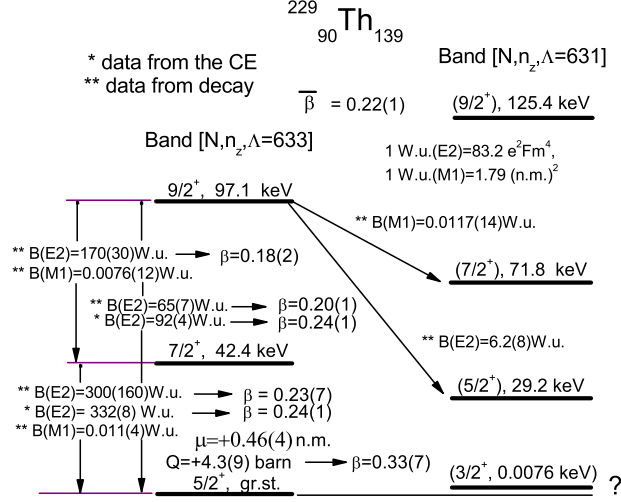


Figure 1: Low-lying levels in  $^{229}\text{Th}$

In (1) and (2)  $\chi_K$  are Nilsson orbitals [10] that represent the decomposition of the single-particle functions of the axially-symmetric deformed potential over the spherical-symmetric functions,  $\Lambda$  and  $s$  are projections of orbital moment and spin on the symmetry axis,  $K = \Lambda + s$ .

We define reduced transition matrix elements and reduced transition rates by the relations

$$\begin{aligned} \langle J_2 M_2 | \hat{m}(\lambda \mu) | J_1 M_1 \rangle &= (-1)^{J_2 - M_2} \begin{pmatrix} J_2 & \lambda & J_1 \\ -M_2 & \mu & M_1 \end{pmatrix} \langle J_2 || \hat{m}(\lambda) || J_1 \rangle, \\ \langle J_2 || \hat{m}(\lambda) || J_1 \rangle &= (-1)^{J_2 - J_1} \langle J_1 || \hat{m}(\lambda) || J_2 \rangle. \end{aligned} \quad (3)$$

$$B(\lambda; J_1 \rightarrow J_2) = \frac{\langle J_2 || \hat{m}(\lambda) || J_1 \rangle^2}{2J_1 + 1}, \quad B(\lambda; J_1 \rightarrow J_2) = \frac{2J_2 + 1}{2J_1 + 1} B(\lambda; J_2 \rightarrow J_1). \quad (4)$$

For  $E2$  transitions we have

$$\hat{m}(E2, \text{core})_\mu^2 = D_{\mu 0}^2(\theta_i) \cdot \frac{3}{4\pi} ZR^2 \cdot \beta |e|, \quad \text{while} \quad \hat{m}(E2, \text{s.p.})_\mu^2 = \sum_\nu D_{\mu\nu}^2(\theta_i) \cdot \hat{m}(E2, \text{intr.})_\nu^2. \quad (5)$$

Then, we obtain

$$\begin{aligned} &\langle \Psi_{K_2}^{J_2} || \hat{m}(E2, \text{core}) + \hat{m}(E2, \text{s.p.}) || \Psi_{K_1}^{J_1} \rangle = \\ &= (-1)^{J_2 - J_1} \sqrt{(2J_1 + 1)} C_{20 J_1 K_1}^{J_2 K_2} \delta(K_1, K_2) \delta(\alpha_1, \alpha_2) \frac{3}{4\pi} |e| \cdot ZR^2 \cdot \beta + \\ &+ (-1)^{J_2 - J_1} \sqrt{\frac{5(2J_1 + 1)}{4\pi}} \cdot \sum_{N \ell \Lambda (1,2)} x_{K_2} (N_2 \ell_2 \Lambda_2 s_2) x_{K_1} (N_1 \ell_1 \Lambda_1 s_1) \cdot (u_1 u_2 - v_1 v_2) \times \\ &\times \sqrt{\frac{2\ell_1 + 1}{2\ell_2 + 1}} C_{20 \ell_1 0}^{\ell_2 0} [\delta(s_1, s_2) C_{2(K_2 - K_1) J_1 K_1}^{J_2 K_2} C_{2(K_2 - K_1) \ell_1 \Lambda_1}^{\ell_2 \Lambda_2} + \\ &+ \delta(s_1, -s_2) (-1)^{J_2 - \ell_2 - 1/2} C_{2(-K_2 - K_1) J_1 K_1}^{J_2 - K_2} C_{2(-K_2 - K_1) \ell_1 \Lambda_1}^{\ell_2 - \Lambda_2}] e_{\text{eff}} \langle 2 | r^2 | 1 \rangle. \end{aligned} \quad (6)$$

In (6)  $u$  and  $v$  are the coefficients of the Bogoliubov transformation, that accounts the superfluid correlations, while  $e_{\text{eff}}$  is the effective quadrupole charge for the odd particle.

Quadrupole moment of state is expressed via the reduced  $E2$  matrix elements by the relation

$$Q_2(J) = \sqrt{\frac{16\pi J(2J-1)}{5(J+1)(2J+1)(2J+3)}} \langle J || \hat{m}(E2) || J \rangle. \quad (7)$$

Consider now  $M1$  transitions. Because of the particle-hole polarization arising from the spin-dependent interactions between the nucleons, “bare” values of gyromagnetic ratios in nuclei renormalize. In addition, this polarization leads to the appearance of the additional tensor term in the single-particle  $M1$  operator which “opens”  $l$ -forbidden transitions in spherical nuclei. In this way, the  $M1$  transition operator in our case reads as

$$\hat{m}(M1)_\mu^1 = \sqrt{\frac{3}{4\pi}} \mu_N \left[ g_R \hat{J} + (g_\ell - g_R) \hat{\ell} + (g_s - g_R) \hat{s} + \delta \hat{\mu}(M1, \text{tens.}) \right]_\mu^1, \quad (8)$$

$$\text{where } \delta \hat{\mu}(M1, \text{tens.})_\mu^1 = \kappa r^2 [Y_2 \otimes \hat{s}]_\mu^1 \cdot \tau_3. \quad (9)$$

In (9)  $\tau_3 = +1$  for neutrons ( $n$ ) and  $\tau_3 = -1$  for protons ( $p$ );  $\kappa = -0.031 \text{ fm}^{-2}$ ;  $g_\ell(p) \approx 1.1$ ,  $g_\ell(n) \approx 0.0$ ,  $g_s(p) = 3.79$ ,  $g_s(n) = -2.04$ ,  $g_R = Z/A = 90/229 = 0.393$ . The values of parameters  $g_\ell$ ,  $g_s$  and  $\kappa$  were defined by us before [11, 12] from the description of magnetic moments as well as  $l$ -allowed and  $l$ -forbidden  $M1$  transition rates in spherical nuclei, both near and far from the closed shells. As a result, we obtain the formula for the reduced  $M1$  transition matrix element:

$$\begin{aligned} & \langle \Psi_{K_2}^{J_2} || \hat{m}(M1, \text{core}) + \hat{m}(M1, \text{s.p.}) || \Psi_{K_1}^{J_1} \rangle = \\ & = g_R \mu_N \delta(K_1, K_2) \delta(J_1, J_2) \delta(\alpha_1, \alpha_2) \sqrt{\frac{3J_1(J_1+1)(2J_1+1)}{4\pi}} + \\ & + (-1)^{J_2-J_1} \sqrt{\frac{3(2J_1+1)}{4\pi}} \mu_N \sum_{N\ell\Lambda s(1,2)} x_{K_2}(N_2 \ell_2 \Lambda_2 s_2) x_{K_1}(N_1 \ell_1 \Lambda_1 s_1) \cdot (u_1 u_2 + v_1 v_2) \times \\ & \times \left\{ (g_\ell - g_R) \sqrt{\ell_1(\ell_1+1)} \delta(n_1, n_2) \delta(\ell_1, \ell_2) \left[ \delta(s_1, s_2) C_{1(K_2-K_1)J_1K_1}^{J_2K_2} \times \right. \right. \\ & \times \left. \left. C_{1(K_2-K_1)\ell_1\Lambda_1}^{\ell_2\Lambda_2} + \delta(s_1 - s_2) (-1)^{J_2-\ell_2-1/2} C_{1(-K_2-K_2)J_1K_1}^{J_2-K_2} C_{1(-K_2-K_1)\ell_1\Lambda_1}^{\ell_2-\Lambda_2} \right] + \right. \\ & + (g_s - g_R) \frac{\sqrt{3}}{2} \delta(n_1, n_2) \delta(\ell_1 \ell_2) \left[ \delta(\Lambda_1, \Lambda_2) C_{1(K_2-K_1)J_1K_1}^{J_2K_2} C_{1(K_2-K_1)1/2 s_1}^{1/2 s_2} + \right. \\ & + \left. \delta(\Lambda_1, -\Lambda_2) (-1)^{J_2-\ell_2-1/2} C_{1(-K_2-K_1)J_1K_1}^{J_2-K_2} C_{1(-K_2-K_1)1/2 s_1}^{1/2 -s_2} \right] - \\ & - \kappa \langle 2 | r^2 | 1 \rangle \left[ C_{1(K_2-K_1)J_1K_1}^{J_2K_2} \langle \ell_2 \Lambda_2 1/2 s_2 || [Y_2 \otimes \hat{s}]_{(K_2-K_1)}^1 | \ell_1 \Lambda_1 1/2 s_1 \rangle + \right. \\ & \left. + (-1)^{J_2-\ell_2-1/2} C_{1(-K_2-K_1)J_1K_1}^{J_2-K_2} \langle \ell_2 - \Lambda_2 1/2 - s_2 || [Y_2 \otimes \hat{s}]_{(-K_2-K_1)}^1 | \ell_1 \Lambda_1 1/2 s_1 \rangle \right] \Big\}. \end{aligned} \quad (10)$$

Here,  $K_1 = \Lambda_1 + s_1$ ,  $K_2 = \Lambda_2 + s_2$ , while

$$\begin{aligned} \langle \ell_2 \Lambda_2 1/2 s_2 | [Y_2 \otimes \hat{s}]_{\mu}^1 | \ell_1 \Lambda_1 1/2 s_1 \rangle &= \frac{3}{2} \sqrt{\frac{5(2\ell_1 + 1)}{2\pi}} C_{\ell_1 0 2 0}^{\ell_2 0} \times \\ &\times \sum_{j_1 j_2} \sqrt{(2j_1 + 1)} C_{j_1 K_1 1 \mu}^{j_2 K_2} C_{\ell_2 \Lambda_2 1/2 s_2}^{j_2 K_2} C_{\ell_1 \Lambda_1 1/2 s_1}^{j_1 K_1} \begin{Bmatrix} \ell_2 & 1/2 & j_2 \\ \ell_1 & 1/2 & j_1 \\ 2 & 1 & 1 \end{Bmatrix}, \quad \mu = \Lambda_2 + s_2 - \Lambda_1 - s_1; \end{aligned} \quad (11)$$

Magnetic moments of states are defined by the relation

$$\mu_J = \sqrt{\frac{4\pi J}{3(J+1)(2J+1)}} \langle J || \hat{m}(M1) || J \rangle. \quad (12)$$

For the  $E2$  transitions between the states of the same rotational band, we may in formula (6) take into account only collective part of the matrix element, as the single-particle one gives only a small contribution. Then, we have standard formulas for the quadrupole moments of states and for the transition rates [7, 9], where the result depends only on the deformation parameter  $\beta$  and the entering values of  $J$  and  $K$ :

$$Q_2(J, K) = \frac{3K^2 - J(J+1)}{(J+1)(2J+3)} Q_0; \quad Q_2(K=J) = \frac{J(2J-1)}{(J+1)(2J+3)} Q_0; \quad Q_0 = \frac{3}{\sqrt{5\pi}} |e| Z R^2 \cdot \beta. \quad (13)$$

$$B(E2; J+1, K \rightarrow J, K) = \frac{3K^2(J+1+K)(J+1-K)}{J(J+1)(J+2)(2J+3)} \cdot \frac{5}{16\pi} Q_0^2, \quad (14)$$

$$B(E2; J+2, K \rightarrow J, K) = \frac{3(J+2+K)(J+1+K)(J+2-K)(J+1-K)}{(2J+2)(2J+3)(J+2)(2J+5)} \cdot \frac{5}{16\pi} Q_0^2. \quad (15)$$

By using experimental data shown in Fig.1 and formulas (13)–(15), one can easily define the magnitude of the deformation parameter  $\beta$  which average value turns out to be  $\bar{\beta} \approx 0.22$ . This is close to the magnitude of  $\beta$ , that corresponds to maximal value of the binding energy  $B$  in  $^{229}\text{Th}$  obtained in calculations [13], which were performed in the Hartree–Fock–Bogoliubov approach with the Gogny interaction. This value of  $\beta$  was used by us in our calculations that involve the “intrinsic” function  $\chi$ .

Consider now transitions between the states of different bands  $|(J_1, J_1')K_1\rangle \rightarrow |(J_2, J_2')K_2\rangle$ , where the initial as well as final states have different values of  $(J, J')$ , but the same values of  $K$ . We see from formula (6) that in case of the  $E2$ -transitions matrix element contains the multiple  $(u_1 u_2 - v_1 v_2)$ , which value is very sensitive to small variation of the single-particle scheme, especially when the entering single-particle orbitals are close to the Fermi level. This is just the case under consideration. In addition, the value of the effective quadrupole charge  $e_{\text{eff}}$  is rather indefinite here, as it is not clear, what part of the quadrupole transition strength should be included in the single-particle mode after taking into account rotation of the core in the obvious way. Thus, direct calculations of the  $E2$  transition matrix elements are not trustworthy here.

However, one can easily see from formulas (6) and (10), that if the multipolarity of radiation  $\lambda$  satisfies the condition  $K_1 + K_2 > \lambda$ , as it takes place if we consider  $E2$  and  $M1$  transitions between the bands [633] and [631], then we have the relation [14]

$$B(\lambda; J'_1 K_1 \rightarrow J'_2 K_2) = \frac{[C_{\lambda(K_2-K_1)J'_1 K_1}^{J'_2 K_2}]^2}{[C_{\lambda(K_2-K_1)J_1 K_1}^{J_2 K_2}]^2} B(\lambda; J_1 K_1 \rightarrow J_2 K_2). \quad (16)$$

As we know from the experiment the value of  $B(E2; J_1 = 9/2, K_1 = 5/2 \rightarrow J_2 = 5/2, K_2 = 3/2) = 6.2(8)$  W.u., we can define in this way all interband  $E2$ -transition matrix elements.

The situation is different in case of  $M1$  transitions. Here, both collective and single-particle parts of the  $M1$  transition matrix element (10) give comparable contributions even in cases of transitions within the same rotational band. In this case, multiple  $(u_1 u_2 + v_1 v_2)$  is close to unity, while the values of  $g_s$  and  $\kappa$  are known. Thus, calculations of  $M1$  transition matrix elements were performed in the obvious way, both for interband transitions and for transitions within the same band.

Results of our calculations of the  $E2$  and  $M1$  electromagnetic characteristics of the  $^{229}\text{Th}$  are shown in Tables 1–3. As one can see from Table 1, the magnitude  $B(M1; 9/2, 5/2 \rightarrow 7/2, 3/2)$  obtained in our calculations is about four times less than the average experimental value shown in [5]. Note however that different experimental values of this quantity differ from each other tenfold more than experimental errors. One can obtain in our calculations average value [5] only if we use  $g_s(n) \approx g_s(n)_{\text{free}}$ , which contradicts generally established conception. Note that if we borrow the value of the  $M1$  single-particle transition matrix element  $\langle \chi_{5/2} | \hat{m}(M1, s.p.) | \chi_{5/2} \rangle$  from the experimental data on the  $|9/2, 5/2\rangle \rightarrow |7/2, 5/2\rangle$  and  $|7/2, 5/2\rangle \rightarrow |5/2, 5/2\rangle$   $M1$  transitions, we in the best cases (by taking the proper sign of the matrix element) have the worse agreement with the experiment on the value of the ground-state magnetic moment of  $^{229}\text{Th}$ , as compared to results of direct calculations.

By using data on transition rates shown in Table 1,  $B(M1; 3/2, 3/2 \rightarrow 5/2, 5/2) = 0.0108 \mu_N^2$  and  $B(E2; 3/2, 3/2 \rightarrow 5/2, 5/2) = 8.0$  W.u., and the values of the conversion coefficients for the 0.0076 keV  $\gamma$ -transition [15] (also the private communication of M.B. Trzhaskovskaya), we find the half-lives for this transition equal to  $T_{1/2}(M1) = 5.9 \cdot 10^{-6}$  s and  $T_{1/2}(E2) = 2.7 \cdot 10^{-3}$  s (including electron conversion). Here, conversion coefficients are very large:  $\alpha_{tot}^{M1}(0.0076 \text{ keV}) \approx 1.4 \cdot 10^9$  and  $\alpha_{tot}^{E2}(0.0076 \text{ keV}) \approx 1.2 \cdot 10^{16}$ . It is important that at such small transition energies, conversion coefficients rapidly grow with decrease of the transition energy (approximately,  $\alpha_{tot}^{M1} \sim 1/(\Delta E)^{3-\epsilon}$  and  $\alpha_{tot}^{E2} \sim 1/(\Delta E)^{5-\epsilon}$ , where  $\epsilon \sim 0.05$ ). *As a result, the half-life of the state of interest at such small transition energies in practice does not depend on energy, but only on the transition matrix element.* In [16, 17] one can find other evaluations of the magnitude of  $T_{1/2}(3/2, 3/2 \rightarrow 5/2, 5/2)^2$ .

Below, we discuss the problem of population of the above-mentioned isomeric state by the method different from  $\alpha$  and  $\beta$ -decays. In the paper [19], authors proposed the method which employs synchrotron radiation, while in [20] the authors suggested pumping  $^{229m}\text{Th}$  by the hollow-cathode discharge. Here, we consider the chance for excitation of the isomeric state in

---

<sup>2</sup>The latest theoretical estimations for transition rates in  $^{229}\text{Th}$  are in [18]

the Coulomb excitation, the process that was proposed for the first time in [21] and elaborated in details in [22].

Table 1: Reduced transition rates for the interband  $E2$  and  $M1$  transitions between the low-lying levels of the bands  $[N_1 n_z(1)\Lambda_1] = [633]$  and  $[N_2 n_z(2)\Lambda_2] = [631]$  in  $^{229}\text{Th}$ . Calculations of the  $E2$  transition rates, shown in the W.u., were based on formula (16), where the experimental value of  $B(E2; J_1 = 9/2 K_1 = 5/2 [633] \rightarrow J_2 = 5/2 K_2 = 3/2 [631]) = 6.2(8)$  was used as the normalization factor. Here,  $\text{W.u.}(E2) = 83.2 e^2\text{fm}^4$ . Results on the  $B(M1)$  values are shown in the units of  $\mu_N^2$  ( $1 \text{ W.u.}(M1) = 1.79 \mu_N^2$ ), and they were obtained by calculations basing on formula (10) with  $\beta = 0.2$ ,  $g_s(n, \text{eff}) = -2, 04$  and  $\kappa = -0.031 \text{ fm}^{-2}$ .

$E, M(\lambda)$	$J_1 K_1$	$J_2 K_2$	$B(1 \rightarrow 2)$	$E, M(\lambda)$	$J_1 K_1$	$J_2 K_2$	$B(1 \rightarrow 2)$
$E2$	9/2 3/2	5/2 5/2	0.53	$E2$	3/2 3/2	5/2 5/2	8.0
$E2$	9/2 3/2	7/2 5/2	4.6	$M1$	9/2 3/2	7/2 5/2	0.00072
$E2$	9/2 3/2	9/2 5/2	3.9	$M1$	9/2 3/2	9/2 5/2	0.00460
$E2$	9/2 5/2	5/2 3/2	6.2 [6.2(8)]	$M1$	9/2 5/2	7/2 3/2	0.00506 [0.0209(25)]
$E2$	9/2 5/2	7/2 3/2	0.11	$M1$	7/2 3/2	5/2 5/2	0.00039
$E2$	7/2 3/2	5/2 5/2	3.3	$M1$	7/2 3/2	7/2 5/2	0.00413
$E2$	7/2 3/2	7/2 5/2	5.7	$M1$	7/2 5/2	5/2 3/2	0.00581
$E2$	7/2 5/2	3/2 3/2	5.3	$M1$	5/2 3/2	5/2 5/2	0.00310
$E2$	7/2 5/2	5/2 3/2	0.22	$M1$	3/2 3/2	5/2 5/2	0.01080
$E2$	5/2 3/2	5/2 5/2	8.0				

For the  $E2$  Coulomb excitation we have

$$\frac{d\sigma_{E2}(\xi, \vartheta)}{d\Omega} = \left( \frac{Z_1 e^2}{\hbar v} \right)^2 \frac{1}{a^2} B(E2 \uparrow) \frac{df_{E2}(\xi, \vartheta)}{d\Omega},$$

$$a \approx 0.072 \frac{Z_1 Z_2}{E_1 (\text{MeV})} (1 + A_1/A_2) \cdot 10^{-12} \text{cm}, \quad \xi = \frac{Z_1 Z_2 A_1^{1/2} (1 + A_1/A_2) \Delta E}{12.65 (E_1 - 1/2 \cdot \Delta E)^{3/2}}. \quad (17)$$

Here,  $A_1$ ,  $Z_1$  and  $E_1$  refer to the projectile,  $E_1$  and  $\Delta E$  are energy in the laboratory system and the excitation energy in MeV,  $a$  is half the distance of the closest drawing in the backward scattering. Functions  $f_{E2}(\xi, \vartheta)$  are expressed [22] via integrals over trajectories. If  $\Delta E/E_1 = 0$ , then we obtain

$$\frac{df_{E2}(\xi = 0, \vartheta)}{d\Omega} = \frac{\pi}{25} \left\{ \left[ 1 - \frac{\pi - \vartheta}{2} \tan \frac{\vartheta}{2} \right]^2 \cdot \frac{1}{\cos^4 \vartheta/2} + \frac{1}{3} \right\}. \quad (18)$$

In a general case, we have [22]

$$\sigma_{E2}(\xi) = 4.78 \frac{A_1 E_{kin}(A_1, \text{MeV}) B(E2 \uparrow, \text{barn}^2)}{Z_2^2 (1 + A_1/A_2)^2} f_{E2}(\xi) \text{ barn}, \quad (19)$$

where  $f_{E2}(\xi = 0) = 0.895$ .

Table 2: Reduced  $E2$  and  $M1$  transition rates between the levels inside the  $K = 5/2$  and  $K = 3/2$  bands. Here, the  $B(E2)$  values are in the Weisskopf units and were calculated by using  $\bar{\beta} = 0.22$ . Numbers in square brackets show experimental results [4, 5]. The  $M1$  rates are in the units of  $\mu_N^2$ , and they were calculated by using  $g_s(n, \text{eff}) = -2.04$  and  $\kappa = -0.031 \text{ fm}^{-2}$ .

$E, M(\lambda)$	$J_1 K_1$	$J_2 K_2$	$B(1 \rightarrow 2)$	$E, M(\lambda)$	$J_1 K_1$	$J_2 K_2$	$B(1 \rightarrow 2)$
$E2$	9/2 3/2	5/2 3/2	167	$E2$	5/2 3/2	3/2 3/2	267
$E2$	9/2 3/2	7/2 3/2	109	$M1$	9/2 3/2	7/2 3/2	0.0583
$E2$	9/2 5/2	5/2 5/2	78 [85(4)]	$M1$	9/2 5/2	7/2 5/2	0.0386 [0.0136(21)]
$E2$	9/2 5/2	7/2 5/2	236 [170(30)]	$M1$	7/2 3/2	5/2 3/2	0.0521
$E2$	7/2 3/2	3/2 3/2	111	$M1$	7/2 5/2	5/2 5/2	0.0266 [0.0197(72)]
$E2$	7/2 3/2	5/2 3/2	167	$M1$	5/2 3/2	3/2 3/2	0.0389
$E2$	7/2 5/2	5/2 5/2	279 [330(8)]				

Table 3: Electric quadrupole and magnetic dipole moments of the lowest states of  $^{229}\text{Th}$ . Here, by calculation of quadrupole moments we used averaged value of  $\bar{\beta} = 0.22$ , while by calculation of magnetic moments we used  $\beta = 0.2$ ,  $g_s(n, \text{eff}) = -2.04$  and  $\kappa = -0.031 \text{ fm}^{-2}$ .

Quantity( $J, K$ )	Exp.	Calc.	Quantity( $J, K$ )	Exp.	Calc.
$Q_2(5/2, 5/2)$	+4.3(9) barn	+2.9 barn	$Q_2(3/2, 3/2)$	–	+1.6 barn
$\mu(5/2, 5/2)$	+0.46(4) $\mu_N$	+0.47 $\mu_N$	$\mu(3/2, 3/2)$	–	+0.12 $\mu_N$

For the  $M1$  Coulomb excitation we have

$$\frac{d\sigma_{M1}(\xi, \vartheta)}{d\Omega} = \left( \frac{Z_1 e^2}{\hbar c} \right)^2 \frac{\lambda_c(p)^2}{4} B(M1 \uparrow) \frac{df_{M1}(\xi, \vartheta)}{d\Omega}, \quad \lambda_c(p) = \frac{\hbar}{m_p c}. \quad (20)$$

For  $\xi = 0$  we obtain

$$\frac{df_{M1}(\xi = 0, \vartheta)}{d\Omega} = \frac{16\pi}{9} \frac{[1 - (\pi - \vartheta)/2 \cdot \tan \vartheta/2]^2}{\sin^2 \vartheta}. \quad (21)$$

We see from Eq.(21), that by  $\Delta E \rightarrow 0$  (as in our case) and  $\vartheta \rightarrow 0$  the total cross section logarithmically diverges. At the same time, the probability of the  $M1$  excitation by  $\xi = 0$ ,  $P(M1, \xi = 0, \vartheta) = d\sigma(M1, \vartheta)/d\sigma(\text{Coul}, \vartheta) \sim \vartheta^2$  by  $\vartheta \rightarrow 0$ . Thus, the divergence of the  $M1$  cross section at  $\vartheta \rightarrow 0$  is due only to the divergence of the Coulomb scattering at  $\vartheta \rightarrow 0$ , in this case the the colliding nuclei are far from each other, and the Coulomb interaction between nuclei is really screened by the electron clouds. Really, almost all electron charge of atom is located at distances less than the Bohr radius  $R_B = \hbar^2/(m_e e^2)$ . In this way, we should exclude intervals more than  $R_{\text{max}}$ , i.e. exclude scattering angles less than  $\vartheta_{\text{min}}$ , where

$$\vartheta_{\text{min}} = 2 \arcsin \left( \frac{1}{R_{\text{max}}/a - 1} \right) \approx \frac{2a}{R_{\text{max}}}, \quad R_{\text{max}} \approx 2R_B. \quad (22)$$

Table 4: Comparison between the cross sections  $\sigma$  and the “effective” cross sections  $\sigma_{\text{eff}}$  for the Coulomb excitation of the  $^{229}\text{Th}$  levels by protons and  $\alpha$ -particles.

Level	Energy keV	Protons, 6 MeV		Protons, 10 MeV		$^4\text{He}$ , 10 MeV	
		$\sigma$ , barn	$\sigma_{\text{eff}}$ , barn	$\sigma$ , barn	$\sigma_{\text{eff}}$ , barn	$\sigma$ , barn	$\sigma_{\text{eff}}$ , barn
$3/2_1^+$	0.0076	1.389(-4)	1.008(-3)	2.314(-4)	1.679(-3)	9.020(-4)	6.448(-3)
$5/2_2^+$	29.2	2.082(-4)	7.120(-4)	3.463(-4)	1.186(-3)	1.339(-3)	4.545(-3)
$7/2_1^+$	42.4	9.696(-3)	1.236(-2)	1.613(-2)	2.058(-2)	6.202(-2)	7.894(-2)
$7/2_2^+$	71.8	1.151(-4)	2.977(-4)	1.916(-4)	4.966(-4)	7.316 (-4)	1.890(-3)
$9/2_1^+$	97.1	3.370(-3)	3.371(-3)	5.620(-3)	5.621(-3)	2.138(-2)	2.139(-2)
$9/2_2^+$	125.4	2.291(-5)	2.291(-5)	3.831(-5)	3.831(-5)	1.429(-4)	1.429(-4)

Then, we obtain

$$\sigma_{M1} = 0.589 \cdot 10^{-8} Z_1^2 B(M1 \uparrow) f_{M1}(\xi = 0, \vartheta_{\min}) \text{ barn} . \quad (23)$$

Here,  $B(M1)$  is in the units of  $\mu_N^2$  and

$$f_{M1}(\xi = 0, \vartheta_{\min}) = \frac{32 \pi^2}{9} \int_{\vartheta_{\min}}^{\pi} \frac{[1 - (\pi - \vartheta)/2 \cdot \tan \vartheta/2]^2}{\sin \vartheta} d\vartheta . \quad (24)$$

For  $\vartheta_{\min 1,2}$  less than  $1^0$  we have

$$f_{M1}(\xi = 0, \vartheta_{\min 1}) \approx f_{M1}(\xi = 0, \vartheta_{\min 2}) + \frac{32\pi^2}{9} \ln \left( \frac{\vartheta_{\min 2}}{\vartheta_{\min 1}} \right) . \quad (25)$$

For protons and  $\alpha$ -particles with energies 10 MeV bombarding  $^{229}\text{Th}$ ,  $\vartheta_{\min} \sim 0.1^0$  and  $f_{M1}(\xi = 0, \vartheta_{\min} = 0.1^0) = 186$ . The corresponding cross section is negligible as compared to the  $E2$  excitation, this statement is even more valid for excitation of high-lying states, for which the magnitude of  $f_{M1}$  rapidly decreases, see also [23]. Thus, all levels considered by us here, are populated in the Coulomb excitation by means of the  $E2$  transitions.

One should allow for the fact that settlement of the lowest  $3/2^+$  level may happen not only due to the direct Coulomb excitation from the ground state, but also due to the discharging of the excited higher-lying states. This process is very important as many of these states are actively excited due to large  $B(E2)$  values. In this way, we took into account excitation of all levels shown in Fig.1, as well as all possible  $E2$  and  $M1$  transitions between them. Corresponding  $B(E2)$  and  $B(M1)$  values were borrowed by us from Tables 1 and 2, while the necessary conversion coefficients were borrowed from [24]. Results of our calculations of cross sections are demonstrated in Table 4. Here,  $\sigma$  corresponds to the direct excitation, while  $\sigma_{\text{eff}}$  is the effective cross section, that includes settlement of the  $3/2_1^+$  state by  $\gamma$ -transitions from the high-lying levels. One can easily see that the allowance of feeding from the high-lying states leads to considerable increase of population of the isomeric state. Note, that taking into account additional excited states leads to further increase of  $\sigma_{\text{eff}}$  as compared to  $\sigma$ .



For example, let's take the foil of  $^{229}\text{Th}$  with thickness  $d = 10 \mu\text{m}$ . The density  $\rho$  of Th is about  $3 \cdot 10^{22}$  atoms/cm<sup>3</sup>. Suppose that we have constant in time beam of 10 MeV protons with a beam current  $j$  equal to  $1 \mu\text{A}$  ( $\sim 0.6 \cdot 10^{13}$  atoms/s). Then, the counting rate for transitions from the 0.0076 keV level (allowing also for the settlement of this level from the high-lying states that are excited in the process of the Coulomb excitation) is  $N = j \cdot \sigma_{\text{eff}} \cdot \rho \cdot d \approx 3 \cdot 10^5 \text{ s}^{-1}$ . However, this level decays mainly by the electron conversion ( $\alpha_{\text{tot}}^{M1} \approx 1.4 \cdot 10^9$ ). Thus, the counting rate for  $\gamma$ -quanta is only  $N_\gamma \sim 2 \cdot 10^{-4} \text{ s}^{-1}$ , i.e.  $\sim 20 \text{ d}^{-1}$ . However, one should keep in mind that metallic Th is not transparent for "blue"  $\gamma$ -rays. Thus, it is better to use a target from the radiolucent glassy material containing Th atoms.

The author acknowledge M.B. Trzhaskovskaya for discussions and calculations concerning problems of atomic structure, as well as Yu.N. Novikov and A.V. Popov for useful critical remarks.

## References

- [1] B.R. Beck, J.A. Becker, P. Beiersdorfer, et al., Phys. Rev. Lett. **98**, 142501 (2007).
- [2] Lars von der Wense, B. Seiferle, M. Laatiaoui *et al.*, Nature **533**, 47 (2016).
- [3] B. Seiferle, Lars von der Wense and P.G.Thirolf, Phys. Rev. Lett. **118**, 042501 (2017).
- [4] S.J. Goldstein, et al. Phys. Rev. C**40**, 2793 (1989).
- [5] E. Browne, J.K. Tuli, Nucl. Data Sheets **109**, 2657 (2008).
- [6] A. Bohr, Dan. Mat. Fys. Medd. **26**, No. 14 (1952).
- [7] A. Bohr and B. Mottelson, Dan. Mat. Fys. Medd. **27**, No. 16 (1953).
- [8] A. Bohr, *Rotational states of atomic nuclei*, Copenhagen (1954).
- [9] A. Bohr and B. Mottelson, Dan. Mat. Fys. Medd. **30**, No. 1 (1955).
- [10] S.G. Nilsson, Dan. Mat. Fys. Medd. **29**, No. 16 (1955).
- [11] S.A. Artamonov, V.I. Isakov, S.G. Kadmsky *et al.*, Sov. J. Nucl. Phys. **36**, 486 (1982).
- [12] V.I. Isakov, Physics of Atomic Nuclei, **79**, 811 (2016).
- [13] S. Hilaire and M. Girod, Eur. Phys. J., **A33**, 237 (2007); see also [http://phynu.cea.fr/HFB-Gogny\\_eng.htm](http://phynu.cea.fr/HFB-Gogny_eng.htm)
- [14] G. Alaga, K. Alder, A. Bohr, B. Mottelson, Dan. Mat. Fys. Medd. **29**, No 9 (1955).
- [15] F.F. Karpeshin and M.B. Trzhaskovskaya, Phys. Rev. C**76**, 054313 (2007).
- [16] V.F. Strizhov and E.V. Tkalya, Sov.Phys. JETP **72**, 387 (1991).

- [17] E.V. Tkalya, C. Schneider, J. Jeet, and E.R. Hudson, Phys. Rev. C **92**, 054324 (2015).
- [18] Nikolay Minkov and Adriana Pálffy, arXiv:1704.07919v2[nucl.th].
- [19] J. Jeet, Ch. Schneider, S.T. Sullivan, et al., Phys. Rev. Lett. **114**, 253001 (2015).
- [20] N.N. Inamura, T. Mitsugashira, et al., Hyperfine Interactions **162**, 115 (2005).
- [21] K.A. Ter-Martirosyan, Sov. Phys. JETP **22**, 284 (1952).
- [22] K. Alder, A. Bohr, T. Huus, B. Motetlson, and A. Winther, Rev. Mod. Phys. **28**, 432 (1956).
- [23] K. Alder and A. Winther, Dan. Mat. Fys. Medd., **31**, No. 1 (1956).
- [24] T. Kibe'di, N.W. Burrows, M.B. Trzhaskovskaya, et al., Nucl. Instr. and Meth., **A589**, 202 (2008); see also <http://bricc.anu.edu.au/index.php>